REPORT DOCUMENTATION PAGE

Form Approved OMB NO. 0704-0188

1. REPORT DATE (DD-MM-YYYY)	2. REPORT TYPE	3. DATES COVERED (From - To)
07-10-2015	Final Report	18-Aug-2014 - 17-May-2015

4. TITLE AND SUBTITLE
Final Report: Indentation Study of 2D Carbides for Manufacturing Novel Multifunctional Composites

5a. CONTRACT NUMBER
W911NF-14-1-0568

5b. GRANT NUMBER

5c. PROGRAM ELEMENT NUMBER
611102

6. AUTHORS
Yury Gogotsi, Vadym N. Borysiuk, Vadym N. Mochalin

5d. PROJECT NUMBER

5e. TASK NUMBER

5f. WORK UNIT NUMBER

7. PERFORMING ORGANIZATION NAMES AND ADDRESSES
Drexel University
Office of Research
3201 Arch Street, Suite 100
Philadelphia, PA 19104 -2875

8. PERFORMING ORGANIZATION REPORT NUMBER

9. SPONSORING/MONITORING AGENCY NAME(S) AND ADDRESS (ES)
U.S. Army Research Office
P.O. Box 12211
Research Triangle Park, NC 27709-2211

10. SPONSOR/MONITOR'S ACRONYM(S)
ARO

11. SPONSOR/MONITOR'S REPORT NUMBER(S)
66237-MS-II.2

12. DISTRIBUTION AVAILIBILITY STATEMENT
Approved for Public Release; Distribution Unlimited

13. SUPPLEMENTARY NOTES
The views, opinions and/or findings contained in this report are those of the author(s) and should not contrued as an official Department of the Army position, policy or decision, unless so designated by other documentation.

14. ABSTRACT
Two-dimensional (2D) materials beyond graphene are attracting much attention. Recently, we discovered a new family of 2D transition metals carbides and carbonitrides called MXenes. Unlike graphene, MXene family is very diverse and to date the number of synthesized MXenes reaches 17 members, including Ti3C2, Nb2C, V2C, Ta4C3, Cr2TiC2, Mo2TiC2, etc. Although MXenes have shown very attractive electrical, electrochemical properties, their mechanical properties are yet to be characterized. There are neither experimental measurements reported in literature nor prediction of strength and fracture modes for single layer MXenes. In this 9-month research study, we

15. SUBJECT TERMS
Nanocarbide,MXenes,two-dimensional

16. SECURITY CLASSIFICATION OF:			17. LIMITATION OF ABSTRACT	15. NUMBER OF PAGES	19a. NAME OF RESPONSIBLE PERSON
a. REPORT	b. ABSTRACT	c. THIS PAGE			Yury Gogotsi
UU	UU	UU	UU		19b. TELEPHONE NUMBER 215-895-6446

Report Title

Final Report: Indentation Study of 2D Carbides for Manufacturing Novel Multifunctional Composites

ABSTRACT

Two-dimensional (2D) materials beyond graphene are attracting much attention. Recently, we discovered a new family of 2D transition metals carbides and carbonitrides called MXenes. Unlike graphene, MXene family is very diverse and to date the number of synthesized MXenes reaches 17 members, including Ti3C2, Nb2C, V2C, Ta4C3, Cr2TiC2, Mo2TiC2, etc. Although MXenes have shown very attractive electrical, electrochemical properties, their mechanical properties are yet to be characterized. There are neither experimental measurements reported in literature nor prediction of strength and fracture modes for single-layer MXenes. In this 9-month research study, we took the first steps to investigate MXenes mechanical properties in both theoretical and experimental aspects. Molecular dynamics was used to predict stress-strain curves of all Tin+1Cn MXenes under tensile deformation. In addition, atomic force microscopy on Ti3C2 flakes and nanoindentation on Ti3C2-polymer composite films were performed to experimentally characterize MXenes mechanical properties.

Enter List of papers submitted or published that acknowledge ARO support from the start of the project to the date of this printing. List the papers, including journal references, in the following categories:

(a) Papers published in peer-reviewed journals (N/A for none)

Received	Paper

TOTAL:

Number of Papers published in peer-reviewed journals:

(b) Papers published in non-peer-reviewed journals (N/A for none)

Received	Paper

TOTAL: **1**

Number of Papers published in non peer-reviewed journals:

(c) Presentations

Number of Presentations: 0.00

Non Peer-Reviewed Conference Proceeding publications (other than abstracts):

Received Paper

TOTAL:

Number of Non Peer-Reviewed Conference Proceeding publications (other than abstracts):

Peer-Reviewed Conference Proceeding publications (other than abstracts):

Received Paper

TOTAL:

Number of Peer-Reviewed Conference Proceeding publications (other than abstracts):

(d) Manuscripts

Received Paper

TOTAL:

Number of Manuscripts:

Books

Received Book

TOTAL:

Received	Book Chapter

TOTAL:

Patents Submitted

Patents Awarded

Awards

Graduate Students

NAME	PERCENT_SUPPORTED
FTE Equivalent:	
Total Number:	

Names of Post Doctorates

NAME	PERCENT_SUPPORTED
Babak Anasori	0.00
FTE Equivalent:	**0.00**
Total Number:	**1**

Names of Faculty Supported

NAME	PERCENT_SUPPORTED
FTE Equivalent:	
Total Number:	

Names of Under Graduate students supported

NAME	PERCENT_SUPPORTED
FTE Equivalent:	
Total Number:	

Student Metrics

This section only applies to graduating undergraduates supported by this agreement in this reporting period

The number of undergraduates funded by this agreement who graduated during this period: 0.00

The number of undergraduates funded by this agreement who graduated during this period with a degree in science, mathematics, engineering, or technology fields:..... 0.00

The number of undergraduates funded by your agreement who graduated during this period and will continue to pursue a graduate or Ph.D. degree in science, mathematics, engineering, or technology fields:..... 0.00

Number of graduating undergraduates who achieved a 3.5 GPA to 4.0 (4.0 max scale):..... 0.00

Number of graduating undergraduates funded by a DoD funded Center of Excellence grant for Education, Research and Engineering:..... 0.00

The number of undergraduates funded by your agreement who graduated during this period and intend to work for the Department of Defense 0.00

The number of undergraduates funded by your agreement who graduated during this period and will receive scholarships or fellowships for further studies in science, mathematics, engineering or technology fields: 0.00

Names of Personnel receiving masters degrees

NAME

Total Number:

Names of personnel receiving PHDs

NAME

Total Number:

Names of other research staff

NAME	PERCENT_SUPPORTED

FTE Equivalent:

Total Number:

Sub Contractors (DD882)

Inventions (DD882)

Scientific Progress

Two-dimensional (2D) materials beyond graphene are attracting much attention. Recently, we discovered a new family of 2D transition metals carbides and carbonitrides called MXenes. Unlike graphene, MXene family is very diverse and to date the number of synthesized MXenes reaches 17 members, including Ti3C2, Nb2C, V2C, Ta4C3, Cr2TiC2, Mo2TiC2, etc. Although MXenes have shown very attractive electrical, electrochemical properties, their mechanical properties are yet to be characterized. There are neither experimental measurements reported in literature nor prediction of strength and fracture modes for single-layer MXenes. In this 9-month research study, we took the first steps to investigate MXenes mechanical properties in both theoretical and experimental aspects. Molecular dynamics was used to predict stress-strain curves of all Tin+1Cn MXenes under tensile deformation. In addition, atomic force microscopy on Ti3C2 flakes and nanoindentation on Ti3C2-polymer composite films were performed to experimentally characterize MXenes mechanical properties.

Technology Transfer

Report for Short Term Innovative Research (STIR) Project

Title:
Indentation Study of 2D Carbides for Manufacturing Novel Multifunctional Composites

Fund Number: W911NF-14-1-0568

PI: Prof. Yury Gogotsi, Drexel University

Submitted to: Dr. David M. Stepp
U.S. Army Research Office
AMSRL-RO-PM (Materials Science Division)

Abstract:
Two-dimensional (2D) materials beyond graphene are attracting much attention. Recently, we discovered a new family of 2D transition metals carbides and carbonitrides called MXenes. Unlike graphene, MXene family is very diverse and to date the number of synthesized MXenes reaches 17 members, including Ti_3C_2, Nb_2C, V_2C, Ta_4C_3, Cr_2TiC_2, Mo_2TiC_2, etc. Although MXenes have shown very attractive electrical, electrochemical properties, their mechanical properties are yet to be characterized. There are neither experimental measurements reported in literature nor prediction of strength and fracture modes for single-layer MXenes. In this 9-month research study, we took the first steps to investigate MXenes mechanical properties in both theoretical and experimental aspects. Molecular dynamics was used to predict stress-strain curves of all $Ti_{n+1}C_n$ MXenes under tensile deformation. In addition, atomic force microscopy on Ti_3C_2 flakes and nanoindentation on Ti_3C_2-polymer composite films were performed to experimentally characterize MXenes mechanical properties.

Statement of the Problem Studied

In 2011, we discovered a new, large family of two-dimensional (2D) transition metal carbides and carbonitrides, named MXenes.[1] Although it has been only four years since the first report on this new 2D materials, MXenes are being studied in many countries including China,[2-22] Russia,[23-26] Japan,[27-29] Germany, France,[30,31] Canada,[32] South Korea,[33,34] Singapore,[35] Iran,[36] Sweden,[37] UK,[38] US[39] and Saudi Arabia[40,41]. Despite the large number of research groups investigating different properties of MXenes, no research has been done on their mechanical properties. This can be due to their atomically thin structure, which make the mechanical properties investigation much more challenging compared to 3D materials. Due to this fact, atomic force microscopy (AFM) has been the best technique to study 2D materials, such as graphene or MoS_2.[42-45] Implementation of such technique to MXenes presents even a harder challenge because of a smaller lateral size of the sheets that are currently produced.[46] Besides that, MXenes sheet surfaces are terminated by O, OH and fluorine (F) functional groups, which make the experimental investigation of elastic properties more challenging. Therefore, the mechanical characterization of MXenes is lacking and the only information available was obtained from theoretical (modeling) studies.[47-49]

In this short-term innovative research (STIR) study, we targeted MXenes' mechanical properties from both theoretical and experimental perspectives.

i) For the theoretical part, we utilized molecular dynamics (MD) for the first time to study the mechanical properties of 2D $Ti_{n+1}C_n$ MXenes. The aim of this work was to calculate the structural and elastic properties of the 2D $Ti_{n+1}C_n$ carbides by a large-scale MD simulation and compare them with those obtained from DFT data on single crystal cells.[47] In the absence of a specific force field for MXenes, we aimed to develop a simple and accurate approach that can be used in future investigations of the structural and mechanical properties of the MXenes. Using this approach, we also obtained new insights into fracture modes of MXenes.

We also studied MXenes experimentally from two aspects: a) AFM study on single and few-layer MXene flakes, b) nanoindentation study on MXene composites, which were made by embedding MXene flakes in polymer matrices.

ii) The AFM study of 2D MXene sheets requires preparing freestanding flakes in order to be able to indent them at the atomic level. To do so, we needed a substrate with wells in it, to be able to position a 2D MXene flake on the top of the well. In this short time, we managed to achieve a good progress that will be discussed in the Accomplishments section.
iii) We also studied tribological properties of different MXenes using AFM.
iv) For the nanoindentation study, we embedded MXene flakes in polyvinyl alcohol (PVA) with different mass ratios and fabricated robust, flexible and conductive composites, and measured their elastic moduli and hardness values via nanoindentation.

Summary of Our Most Notable Accomplishments to Date

I. Molecular Dynamic Study of the Mechanical Properties of Two-Dimensional Titanium Carbides $Ti_{n+1}C_n$ (MXenes)[50]

As the first step of mechanical characterization of MXenes, we used large-scale MD for $Ti_{n+1}C_n$ sheets with n = 1, 2, 3. Ti_2C and Ti_3C_2 are among the first MXenes reported,[51,52] while Ti_4C_3 has only been studied computationally.[53] The titanium and carbon atoms were placed at initial positions according to the MXene lattice.[52] In this initial study we did not consider any surface termination of MXene, which may be present when wet chemical synthesis is used.[52] The interatomic distances within five boundary atomic layers on each side in x direction are held fixed during the simulation (Figure 1), while periodic and free boundary conditions were applied in y and z directions respectively. The tensile loading was implemented as in Ref.[54]. During the tensile deformation, the five layers of atoms with fixed interatomic distance on one side of the sample were pulled in the x direction at a constant strain rate of $0.0004\ ps^{-1}$, while the corresponding five layers of atoms on the opposite side of the MXene sheet remained fixed. The lateral (x and y) dimensions of the samples considered in our simulations vary from about 19.50×16.84 nm to 38.71×33.47 nm, where the total number of atoms involved in simulation varies from 12288 to 87808, depending on MXene and system dimensions.

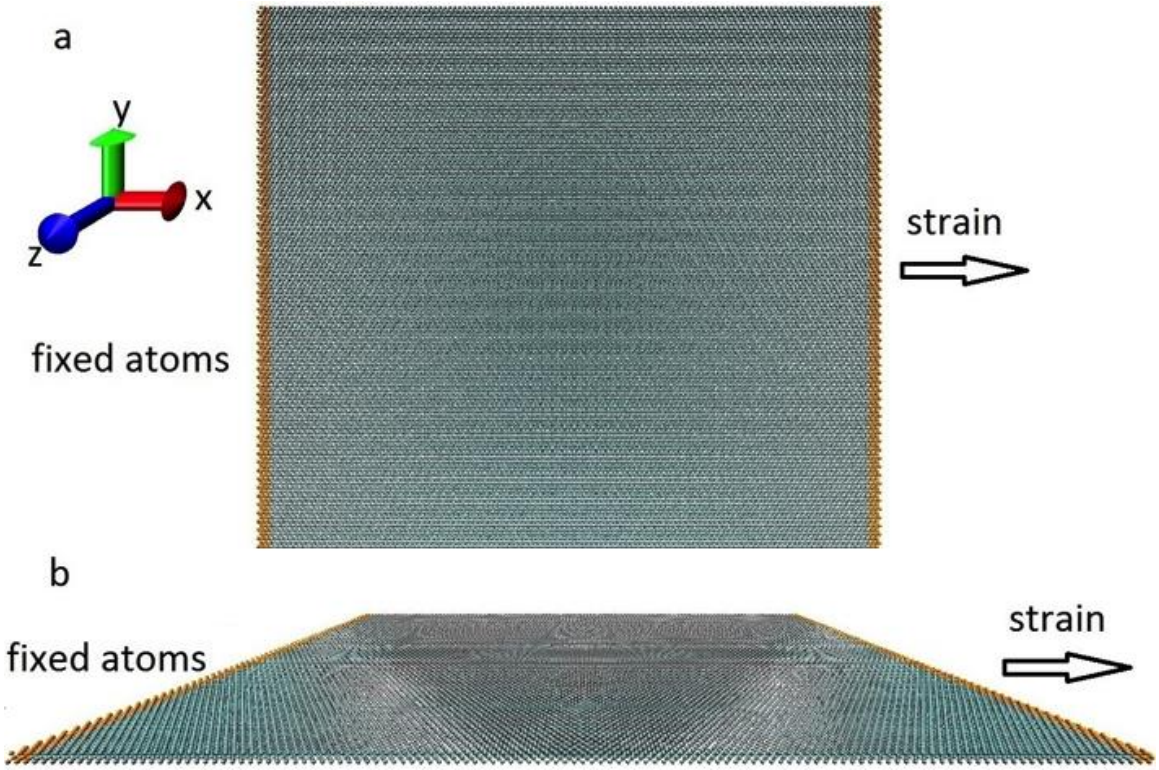

Figure 1. Top (a) and perspective (b) view of the initial configuration of the Ti_2C with the size of 38.71×33.47 nm consisting of 49152 atoms. Five lateral layers of atoms, whose interatomic distances were fixed during simulations, are shown in yellow on both sides.

Interatomic bonding in MAX phases, the precursors of MXenes, is known to be a combination of metallic, covalent, and ionic.[52,55] Therefore, various types of potential energy functions were used to simulate interactions between different types of atoms. As shown before,[56] $Ti_{n+1}C_n$ are metallic conductors, so the metallic type of bonding is supposed to prevail within the Ti layers of the material. With this assumption, the embedded atom method (EAM[57]) was chosen to describe the interaction between titanium atoms in the $Ti_{n+1}C_n$ sheets. The generalized EAM potential is widely used in MD simulations of metal alloys and is well fitted to reproduce the basic material properties.[58,59] Forces between the titanium and carbon atoms are derived from the empirical potential energy function (PEF) parameterized for C-Ti compounds.[60] More details on this study can be found in the paper that is published in the journal of Nanotechnology.[50]

In the beginning of the simulation, all atoms were placed in their initial positions to form an ideal $Ti_{n+1}C_n$ monolayer and the system was equilibrated over $2 \cdot 10^5$ simulation steps. The temperature was maintained at 300 K, using Berendsen thermostat.[61] The snapshots of the simulated samples after equilibration are shown in Figure 2.

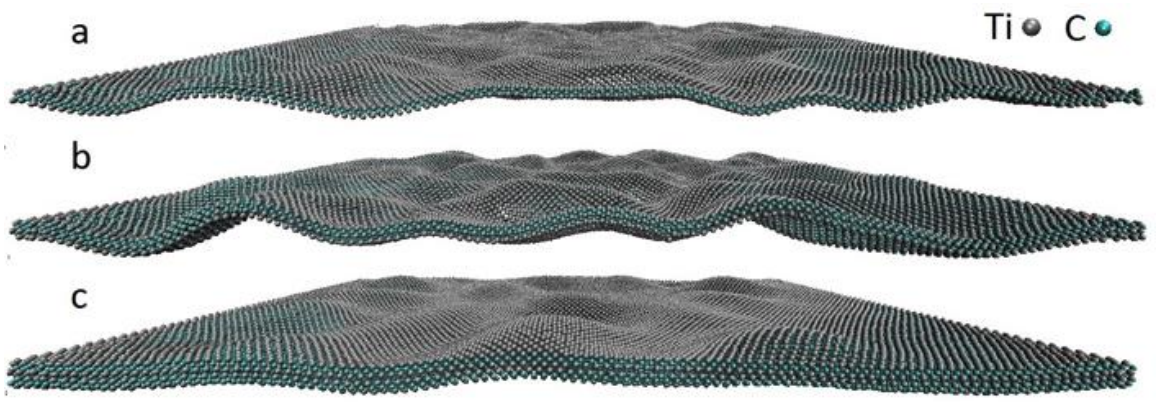

Figure 2. Snapshots of the $Ti_{n+1}C_n$ samples after equilibration at 300 K: a) Ti_2C; b) Ti_3C_2; c) Ti_4C_3.

After the equilibration, the tensile load was applied to the samples, during which the overall stress was calculated. Figure 3 shows the stress-strain curves obtained for the Ti_2C, Ti_3C_2, and Ti_4C_3 samples during their tensile deformation.

All obtained strain-stress curves have a similar shape with an initial linear region, related to elastic deformation. At a higher strain, stress continues to increase up to the threshold point of a yield stress, followed by a sharp drop associated with sample fracture.

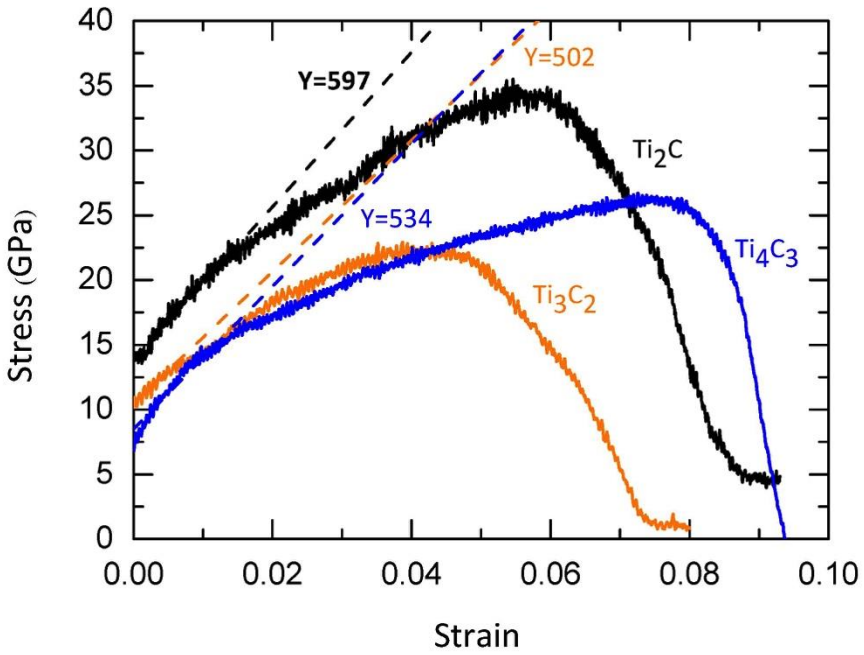

Figure 3. Strain-stress curves obtained for the $Ti_{n+1}C_n$ samples during tensile loading. Dashed lines are extrapolated from the initial linear regions of strain-stress curves.

The Young's moduli obtained by linear fit of the strain-stress curves at the strain $\varepsilon < 0.01$ are 597 , 502 and 534 GPa for Ti_2C, Ti_3C_2, and Ti_4C_3, respectively, with an interpolation error within 10% (Figure 3). These results are close to the published data estimated from first principles calculations.[47] As expected, the highest Young's modulus was observed for Ti_2C MXene sheet and decreased with increasing thickness of MXene layer. Ti_4C_3, which is still to be produced experimentally, showed the highest strain to failure.

Under critical stress all the $Ti_{n+1}C_n$ samples exhibit similar behavior during elastic deformation: no significant defects are formed in the structure and the overall strain of the sample is distributed over the interatomic bonds, resulting in their tension. With further increase in stress, the evolution of the $Ti_{n+1}C_n$ samples is different. The fracture trend of each the $Ti_{n+1}C_n$ samples are shown in the published paper for this study.[50]

To validate the obtained results, the strain-stress simulations were performed at different strain rates for all three $Ti_{n+1}C_n$. Three strain rate values of $0.0002\,ps^{-1}$ 0.0004 ps^{-1} and $0.001\,ps^{-1}$ were used in these simulations. The results of these simulations are shown in Figure 4. As expected, all the strain-stress curves obtained at different strain rates have a linear region of elastic deformation, with the slope in this region being independent on the strain rate.

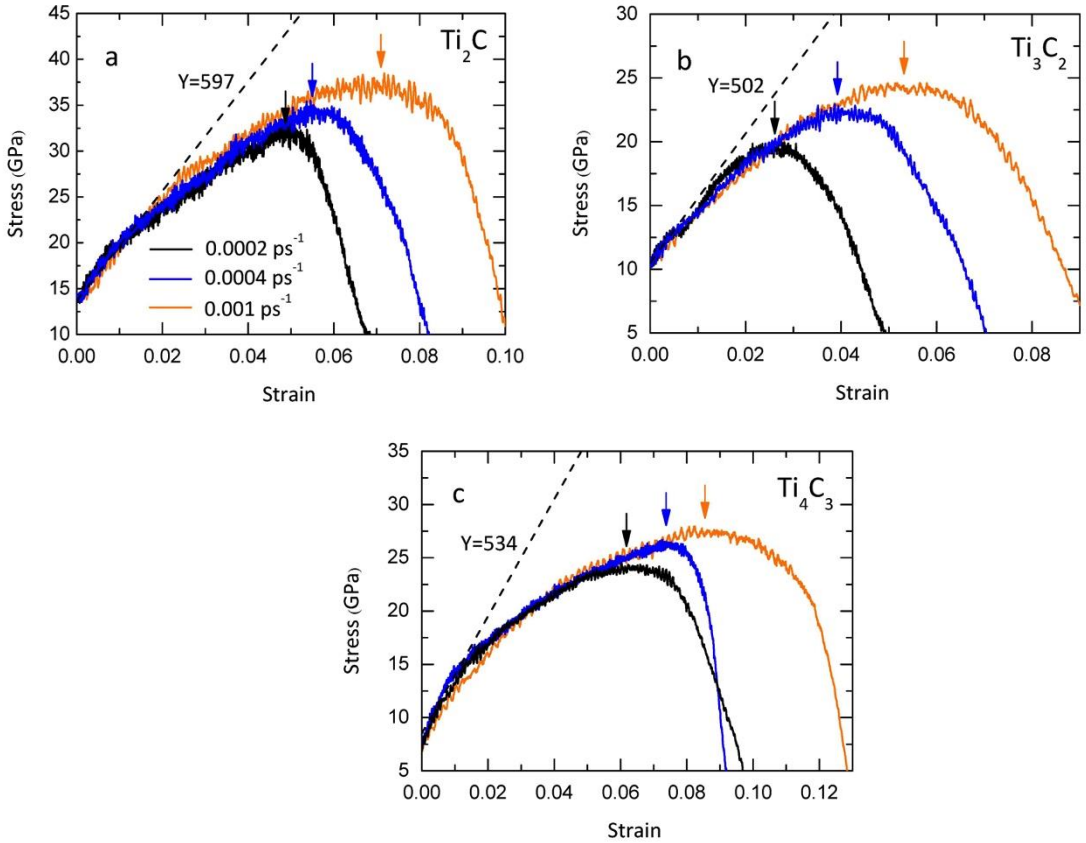

Figure 4. Strain-stress curves for the 2D $Ti_{n+1}C_n$ samples at different strain rates: a) Ti_2C; b) Ti_3C_2; c) Ti_4C_3. Dashed lines indicate the region of linear strain-stress relation. Vertical arrows show the yield points for each curve.

II. AFM indentation study on MXene flakes

Usually the best method to measure mechanical properties of 2D materials is to perform AFM indentation on free-standing flakes.[42-45] In such studies, atomic thick 2D materials such as graphene or MoS_2 were suspended over circular holes in a patterned SiO_2/Si substrate and usually 2D flakes were deposited mechanically, e.g. by putting the 2D flake on an adhesive tape, cleaved and the tape was pressed against the substrate.

As the first step for this study, 5x5mm^2 arrays of circular wells (2 μm diameter and depth of 100nm) were patterned onto a Si substrate with a 300 nm SiO_2 epilayer by nanoimprint lithography and reactive ion etching (wells in Figure 5a).

Ti_3C_2 flakes, the most studied MXene, was prepared by etching the Al layer out from Ti_3AlC_2 MAX phase, its precursor, by dispersing the latter in 6 M HCl with 5 molar equivalent LiF at 30 ºC for 24h. Then the mixture was washed through 5 cycles of distilled water addition, centrifugation (3,500 r.p.m. 2 min for each cycle), and decanting, until the supernatant reached a pH of approximately 6. The final product was dispersed in distilled water (2 g MXene per 0.5 liter of water), deaerated with Ar, followed by sonication for 1 h. The mixture was then centrifuged for 1 h at 3,500 r.p.m., and the supernatant, which was dark green in color was collected and will be referred to as MXene suspension.

Two methods were used to deposit Ti_3C_2 flakes on the substrate, Scotch tape and mechanical shearing. For both methods, 1 drop of the diluted delaminated MXene suspension was filtered. Although MXene flakes are delaminated in the suspension, as soon as they are filtered they tend to restack over each other with secondary bonds between them. For the Scotch tape method, we tried to cleave the MXene stacked flakes after filtraiton with a tape and then deposit a MXene flake on the substrate by pressing the tape against the substrate. We did not achieve any success with this method so far and all the flakes deposited on the substrate were multilayer. Consequently, we came up with the second method, mechanical shearing, in which the filtered droplet of the delaminated Ti_3C_2 suspension was pressed and sheared against the substrate.

After each deposition, optical microscopy was used to find deposited flakes on the substrate and they were marked. The marked substrate was transferred under AFM to measure flakes exact thickness and if a single or few-layer flake was found, measurement was done on it. Figure 5a and b show optical image of the substrate that a thin filtered MXene film was sheared mechanically against it and several MXene flakes are deposited on it. Most of the flakes are smaller than wells diameter (< 2 µm). One large flake was observed in between two well regions (Figure 5a). AFM measurement on different sides of this flakes showed that it was consisted of different numbers of flakes from one side to the other side. When AFM was done at one of its edges (red line in Figure 5d), the thickness was measured to be ~ 1.5 nm (Figure 5e), which corresponds to the thickness of a single layer Ti_3C_2. However, since all the freestanding flakes over the holes were smaller than the well diameter, we have not been able to perform AFM indentation on the MXene flakes.

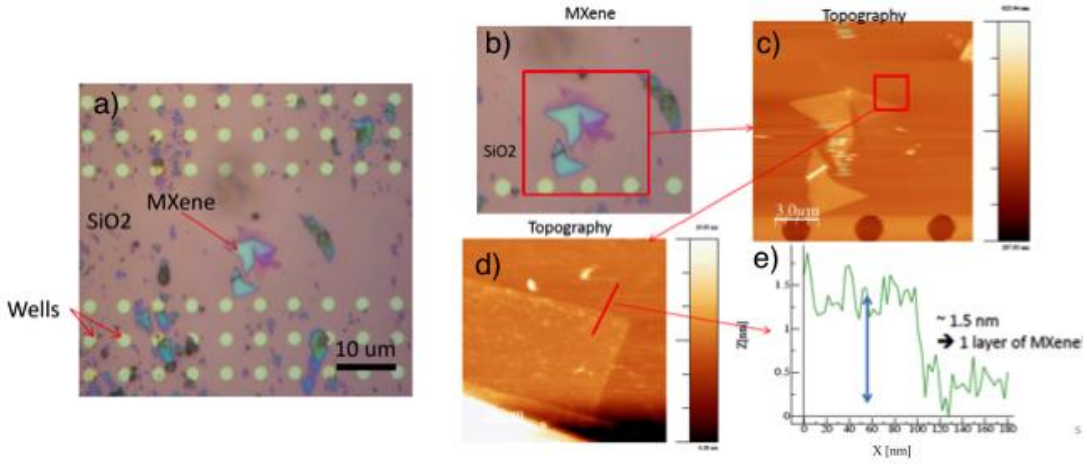

Figure 5. Deposited flakes of Ti_3C_2 on SiO_2 substrate, a, b) optical microscope image showing different flakes of Ti3C2 MXene deposited. Most of the flakes are smaller than the wells. c) AFM topography image of b. d) higher magnification of c. e) AFM scan at the edge of the MXene flake (red line in c) showing the 1.5nm thickness of the flake.

Challenges and ongoing work

Based on our findings with this method, it was clear that we needed smaller well diameters in order to get freestanding MXene flakes. A new substrate with three arrays of

holes with various diameters of 1 µm, 500 nm and 250 nm was fabricated. Tests on this substrate are on going, but further efforts will be required to conduct measurements on single flakes.

III. AFM tribology study on MXene flakes

In addition to AFM indentation on freestanding MXene flakes, we studied tribological properties of the deposited MXene flakes. As discussed earlier, MXenes can have different terminating groups (mostly O, OH and F) depending on the synthesis method. Figure 6 shows a freshly etched Ti_3C_2 particle, with 10 % HF, deposited on the substrate. Friction map (Figure 6b) shows reduction in friction on the Ti_3C_2 MXene. A friction line scan was performed on the MXene flake (black line in Figure 6b) and friction on Ti_3C_2 was measured to be about ~ 2 times less than that of the SiO_2 substrate (Figure 6c). An ongoing study in our group, indicated that surface of the MXene synthesized with this method is mostly terminated by F and less O and OH, which can explain the friction reduction. Moreover, adhesion was measured to be higher than SiO_2 (Figure 6d), which again can be related to the higher concentration of F terminations on the surface.

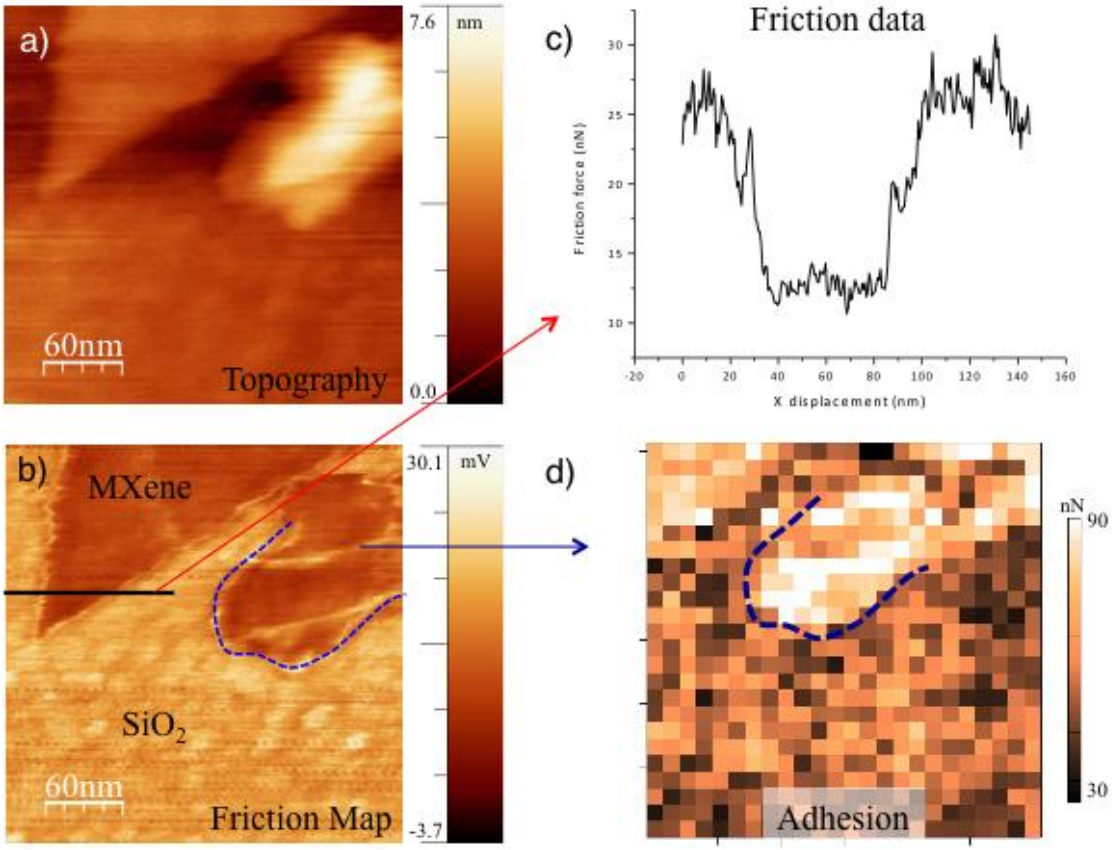

Figure 6. Tribology results of Ti_3C_2 MXene etched with 10 % HF, mostly F terminated, a) AFM topological map on a deposited MXene flake on the substrate. b) Friction map on (a) showing fluorine terminated MXene has different friction than the substrate. c) Friction data on the black line in (b) showing Ti_3C_2 MXene F terminated has about 2 times lower friction that the substrate. d) Adhesion map of the dashed line area in (b), showing higher adhesion on the F terminated MXene.

To further understand the effect of surface termination on tribological properties, we attempted to change the MXene surface termination, by intercalating MXene with dimethyl sulfoxide (DMSO), which in turn reduces the fluorine concentration on the MXene surface. Surface termination of the MXene flakes after being intercalated with DMSO and washed with deionized water, is mostly O and OH groups and less F. These flakes, in contrast to the F terminated ones, has similar friction and adhesion to SiO_2 (Figure 7b, c), showing that flakes terminated mostly with O and OH groups have higher friction and lower adhesion than the mostly F terminated ones.

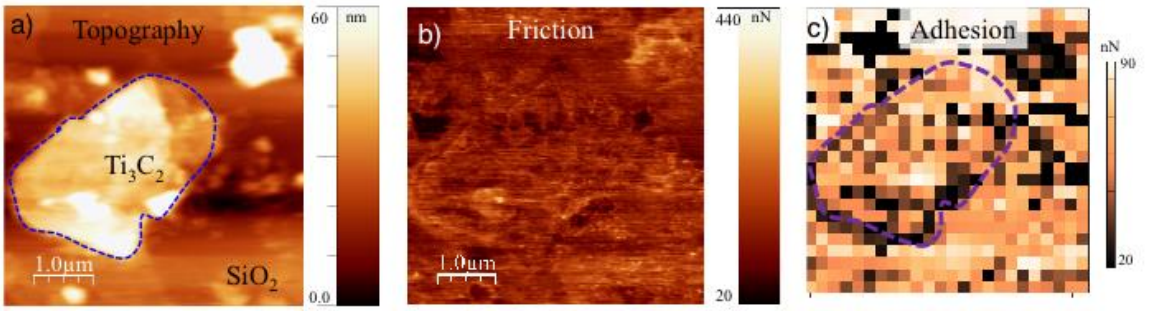

Figure 7. Tribology results of Ti_3C_2 MXene etched with 10 % HF and intercalated with DMSO, a) AFM topological map on a deposited MXene flake on the substrate. b) Friction map on (a) showing MXene intercalated with DMSO (lower F termination) has similar friction to SiO_2. c) Adhesion results of the dashed line area in (a), showing O and OH terminated MXene has similar adhesion to SiO_2 substrate.

Challenges and ongoing work

MXene family, unlike many other 2D materials, can be tuned in terms of the surface termination groups and even the transition metal atoms (M) on their surface. As a future study, we are aiming to further change the surface terminating groups and also study the effect of different M elements on tribological properties of different MXenes.

IV. Nanoindentation study on MXene films and MXene based nanocomposites

In addition to MXene flakes, MXene films and MXene based nanocomposites were fabricated for the first time and their mechanical properties were studied. MXene films were fabricated by vacuum-assisted filtration of Ti_3C_2 colloidal solution (Figure 8a). The MXene colloidal solution synthesis method was explained in section II. In addition, MXene-polyvinyl alcohol (PVA) composites films were fabricated by mixing MXene colloidal solution with a PVA aqueous solution and sonicating for 15 min and vacuum filtration (Figure 8a). Due to the simplicity of synthesis method, any mixing ratio between MXene and PVA can be made. We chose a full range of MXene:PVA weight ratios as 90:10, 80:20, 60:40, 40:60, 10:90 and 5:95. The as-fabricated, additive-free, free-standing Ti_3C_2 and Ti_3C_2-PVA 60:40 films are shown in Figure 8b and c, respectively. The films' thickness can be easily tailored by controlling the MXene content in a given volume of solution. For example, a scanning electron microscope

(SEM) cross-sectional image of a 14 μm thick film is shown in Figure 8d. This image also reveals a well-aligned layered structure throughout the entire film (Figure 8d). Such thin, free-standing, conductive films built of 2D layers, which can be manufactured in aqueous environments and do not require any post treatment but drying, are quite unique. All of the fabricated films, even the 100 % Ti_3C_2 films, are quite flexible and can be readily folded into various shapes without observable damage (Figure 8e).

The electrical conductivities of the Ti_3C_2 films –determined by a standard four-probe technique – are of the order of 2.4 $x10^5$ S/m, a value that is several times higher than that of graphene or carbon nanotube "paper". Note that because the contact resistance between flakes cannot be eliminated, much higher conductivities can be expected for a Ti_3C_2 single layer. Indeed, we have shown that the conductivity of Ti3C2 epitaxial thin film with a nominal thickness of 28 nm is 4.3 x 10^5 S/m [37].

Transmission electron microscopy (TEM) images of Ti_3C_2/PVA (40:60) films (Figure 8f) clearly shows intercalation and confinement of PVA layers in Ti_3C_2 flakes. Since only single-layer of Ti_3C_2 is found in this composites with a high PVA content (Figure 8f), it is reasonable to conclude that primarily single-layer Ti_3C_2 is present in the colloidal solution after delamination and any multilayers MXene that we observed with AFM in the previous section, may be due to restacking of MXene layers during filtration.

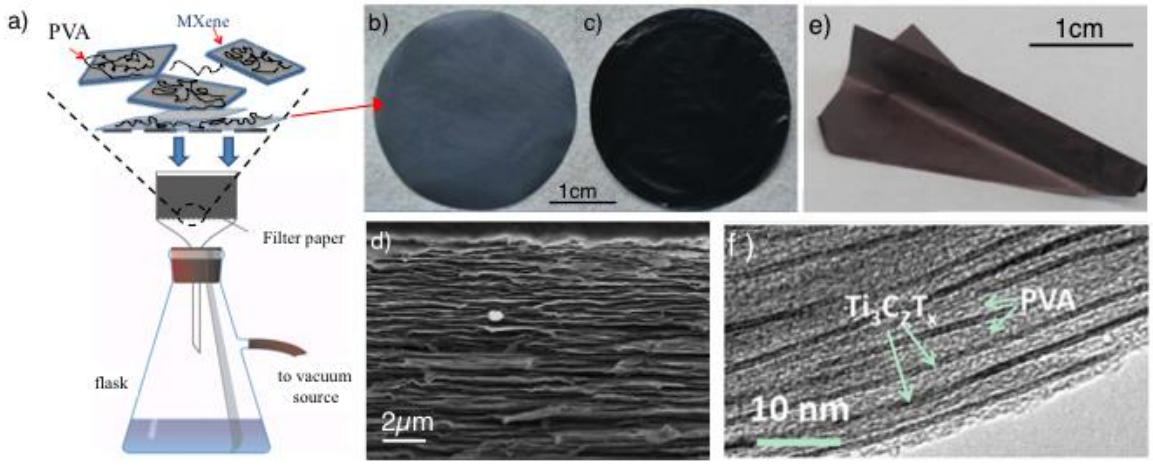

Figure 8. Fabricating MXene-PVA composite films. a) Schematic of filtration of PVA and Ti_3C_2 solution. b and c) Digital image of a free-standing films of b) Ti_3C_2 c) PVA-Ti_3C_2 composite. d) Typical cross-sectional SEM image of a Ti_3C_2 film showing its layered structure of well-stacked flakes. e) To demonstrate mechanical flexibility, a film was folded into a shape of a paper airplane. f) Typical TEM image of 40 wt.% Ti_3C_2/PVA composite film showing intercalation of PVA between Ti_3C_2 flakes.

As noted above, the Ti_3C_2 composite films had sufficient mechanical strength for handling. Spherical nanoindentation with a 1 μm radius tip was used to measure their mechanical properties. Nanoindentation was performed in two directions, face up and edge on (Figure 9a). For the face up tests, as synthesized films were mounted on an aluminum puck sample holder with a wax and indentation was done on the surface of the films (Figure 9a). SEM image of the surface of a Ti_3C_2-PVA (60:40) is shown in Figure 9b. For the edge on tests, films were first mounted edge on in an epoxy resin and after curing the epoxy mount, samples were polished down to 50 nm. SEM image of an edge on 10 wt.% Ti_3C_2-PVA composite is shown in Figure 9c. The spherical indentation mark

on both face on and edge on samples are shown in Figure 9d and e. The elastic moduli and hardness values of the face on tests are almost comparable with each other regardless of the composites' composition (Figure 9f), which can be due to the fact that these films are not fully dense and because of the direction of the tests, they all show the same values. However, for the edge on tests, the indentation results are more reliable, since the indents are on the sections of the films with no visible porosity (Figure 9c). There is a clear trend in both elastic modulus and hardness values of the edge on test and it reaches to its maximum at around 60 wt.% of Ti_3C_2. At 22.7±0.8 GPa, the elastic modulus of the 60 wt.% Ti_3C_2-PVA composite is measured to be more than one order of magnitude higher than that of the 100 % PVA (~ 1.7 GPa). At 5.2 GPa, even addition of 5 wt.% Ti_3C_2 (< 2 vol.% Ti_3C_2) to PVA, tripled the elastic modulus. The same trend is true for the hardness and at ~ 740±30 MPa, hardness reaches to its maximum value for the 60:40 Ti_3C_2-PVA composite.

The general increase in stiffness and hardness of these films indicates that at least some of the stress was transferred to the embedded Ti_3C_2 nanosheets, which in turn implies at least some interfacial bonding between the nanosheets and the PVA. The termination of the Ti_3C_2 by OH groups most probably played an important role here. In addition, the Young's modulus of Ti_3C_2/PVA films can be tailored by controlling the Ti_3C_2 to PVA ratio.

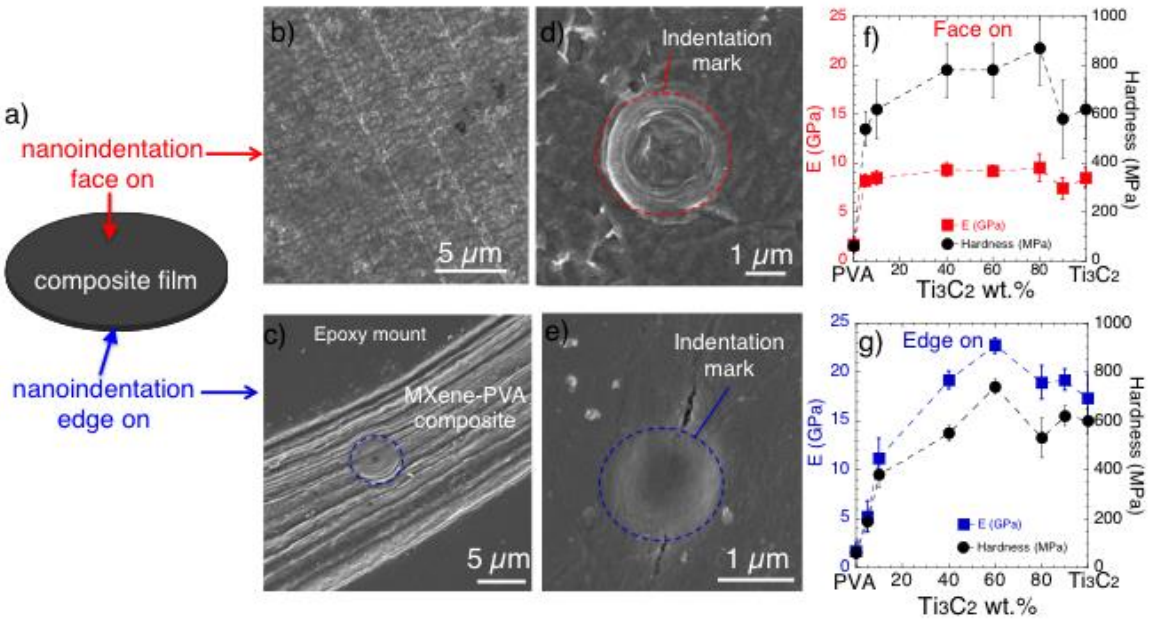

Figure 9. Nanoindentation results on MXene composite films. a) Schematic of nanoindentation on two directions, face on and edge on. b and c) Typical SEM image of b) face on and c) edge on Ti_3C_2-PVA composite film. d and e) SEM image of a nanoindentation mark on a, d) face on and e) edge on Ti_3C_2-PVA composite. f and g) Elastic moduli (E) and hardness values of different films with different MXene loadings tested f) face on and g) edge on. In general, Elastic moduli and hardness in the face on direction are independent of the MXene content. In contrast, for the edge on direction, both E and H are MXene content dependent.

The next step will be to embed MXene flakes into a strong and hard thermoset polymer matrix, such as epoxy resin. We have conducted preliminary experiments,

showing that MXene surface functionalities can lead induce polymerization of the epoxy resin even without an addition of a hardener. Further research is needed to produce mechanically strong composites for armor and other defense applications.

Publications and presentations resulting for this grant:

Papers

1. Borysiuk, V. N.; Mochalin, V. N.; Gogotsi, Y. "Molecular dynamic study of the mechanical properties of two-dimensional titanium carbides $Ti_{n+1}C_n$ (MXenes)" . ***Nanotechnology*** **2015**, 26, 265705.
2. Anasori, B.; Xie, Y.; Beidaghi, M.; Lu, J.; Hultman, L.; Gogotsi, Y.; Barsoum, M. W. "Ordered, two-dimensional, double transition metals carbides (MXenes)". ***ACS Nano*** **2015**, Under Review.
3. Anasori, B.; Liu, X.; Barsoum, M. W.; Carpick, R. W.; Gogotsi, Y.; "Tribological properties of two-dimensional transition metal carbides (MXenes)". In preparation.
4. Anasori, B.; Voigt, C. A.; Barsoum, M. W.; Gogotsi, Y.; "Nanoindentation study on MXene-polyvinyl alcohol (PVA) composites" In preparation.
5. Anasori, B.; Halim, J.; Lu, J.; Voigt, C. A.; Hultman, L.; Barsoum, M. W. "Mo_2TiAlC_2: A new ordered layered ternary carbide". ***Scripta Mater.*** **2015**, 101, 5-7.

Presentation

Anasori, B.; Liu, X.; Barsoum, M. W.; Carpick, R. W.; Gogotsi, Y. "MXenes and MXene-polymer composites: manufacturing, nanoindentation and tribology". **2015 APS/CNM Users Meeting, Argonne National Lab,** May 2015.

References:

1. Naguib, M.; Kurtoglu, M.; Presser, V.; Lu, J.; Niu, J.; Heon, M.; Hultman, L.; Gogotsi, Y.; Barsoum, M. W. Two-Dimensional Nanocrystals Produced by Exfoliation of Ti3AlC2. *Adv. Mater.* **2011**, 23, 4248-4253.
2. Peng, Q.; Guo, J.; zhang, Q.; Xiang, J.; Liu, B.; Zhou, A.; Liu, R.; Tian, Y. Unique Lead Adsorption Behavior of Activated Hydroxyl Group in Two-Dimensional Titanium Carbide. *Journal of the American Chemical Society* **2014**, 136, 4113-4116.
3. Ying, Y.; Liu, Y.; Wang, X.; Mao, Y.; Cao, W.; Hu, P.; Peng, X. Two-Dimensional Titanium Carbide for Efficiently Reductive Removal of Highly Toxic Chromium(VI) from Water. *ACS Applied Materials & Interfaces* **2015**.
4. Li, X.; Fan, G.; Zeng, C. Synthesis of ruthenium nanoparticles deposited on graphene-like transition metal carbide as an effective catalyst for the hydrolysis of sodium borohydride. *International Journal of Hydrogen Energy* **2014**, 39, 14927-14934.
5. Xie, X.; Chen, S.; Ding, W.; Nie, Y.; Wei, Z. An extraordinarily stable catalyst: Pt NPs supported on two-dimensional $Ti_3C_2X_2$ (X = OH, F) nanosheets for oxygen reduction reaction. *Chemical Communications* **2013**, 49, 10112-10114.
6. Xie, X.; Xue, Y.; Li, L.; Chen, S.; Nie, Y.; Ding, W.; Wei, Z. Surface Al leached Ti_3AlC_2 as a substitute for carbon for use as a catalyst support in a harsh corrosive electrochemical system. *Nanoscale* **2014**, 6, 11035-11040.
7. Wang, F.; Yang, C.; Duan, C.; Xiao, D.; Tang, Y.; Zhu, J. An Organ-Like Titanium Carbide Material (MXene) with Multilayer Structure Encapsulating Hemoglobin for a Mediator-Free Biosensor. *J Electrochem Soc* **2014**, 162, B16-B21.
8. Chen, J.; Chen, K.; Tong, D.; Huang, Y.; Zhang, J.; Xue, J.; Huang, Q.; Chen, T. CO_2 and temperature dual responsive "Smart" MXene phases. *Chemical Communications* **2015**, 51, 314-317.
9. Yang, J.; Chen, B.; Song, H.; Tang, H.; Li, C. Synthesis, characterization, and tribological properties of two-dimensional Ti_3C_2. *Crystal Research and Technology* **2014**, 49, 926-932.
10. Li, Z.; Wang, L.; Sun, D.; Zhang, Y.; Liu, B.; Hu, Q.; Zhou, A. Synthesis and thermal stability of two-dimensional carbide MXene Ti_3C_2. *Materials Science and Engineering: B* **2015**, 191, 33-40.
11. Li, J.; Du, Y.; Huo, C.; Wang, S.; Cui, C. Thermal stability of two-dimensional Ti_2C nanosheets. *Ceramics International* **2014**, 41, 2631-2635.
12. Zhao, S.; Kang, W.; Xue, J. MXene nanoribbons. *Journal of Materials Chemistry C* **2015**, 3, 879-888.
13. Zhang, X.; Xue, M.; Yang, X.; Wang, Z.; Luo, G.; Huang, Z.; Sui, X.; Li, C. Preparation and tribological properties of $Ti_3C_2(OH)_2$ nanosheets as additives in base oil. *RSC Advances* **2015**, 5, 2762-2767.
14. Tang, Q.; Zhou, Z.; Shen, P. Are MXenes Promising Anode Materials for Li Ion Batteries? Computational Studies on Electronic Properties and Li Storage Capability of Ti_3C_2 and $Ti_3C_2X_2$ (X = F, OH) Monolayer. *Journal of the American Chemical Society* **2012**, 134, 16909-16916.
15. Zhao, S.; Kang, W.; Xue, J. Role of Strain and Concentration on the Li Adsorption and Diffusion Properties on Ti_2C Layer. *The Journal of Physical Chemistry C* **2014**, 118, 14983-14990.

16. Hu, Q.; Sun, D.; Wu, Q.; Wang, H.; Wang, L.; Liu, B.; Zhou, A.; He, J. MXene: A New Family of Promising Hydrogen Storage Medium. *The Journal of Physical Chemistry A* **2013**, 117, 14253-14260.
17. Zhao, S.; Kang, W.; Xue, J. Manipulation of electronic and magnetic properties of M_2C (M = Hf, Nb, Sc, Ta, Ti, V, Zr) monolayer by applying mechanical strains. *Applied Physics Letters* **2014**, 104, 133106.
18. Gao, Y.; Wang, L.; Li, Z.; Zhou, A.; Hu, Q.; Cao, X. Preparation of MXene-Cu_2O nanocomposite and effect on thermal decomposition of ammonium perchlorate. *Solid State Sciences* **2014**, 35, 62-65.
19. Sun, D.; Wang, M.; Li, Z.; Fan, G.; Fan, L.-Z.; Zhou, A. Two-dimensional Ti_3C_2 as anode material for Li-ion batteries. *Electrochemistry Communications* **2014**, 47, 80-83.
20. Ma, Z.; Hu, Z.; Zhao, X.; Tang, Q.; Wu, D.; Zhou, Z.; Zhang, L. Tunable Band Structures of Heterostructured Bilayers with Transition-Metal Dichalcogenide and MXene Monolayer. *The Journal of Physical Chemistry C* **2014**, 118, 5593-5599.
21. Wang, S.; Li, J.-X.; Du, Y.-L.; Cui, C. First-principles study on structural, electronic and elastic properties of graphene-like hexagonal Ti_2C monolayer. *Computational Materials Science* **2014**, 83, 290-293.
22. Chang, F.; Li, C.; Yang, J.; Tang, H.; Xue, M. Synthesis of a new graphene-like transition metal carbide by de-intercalating Ti_3AlC_2. *Materials Letters* **2013**, 109, 295-298.
23. Shein, I. R.; Ivanovskii, A. L. Graphene-like titanium carbides and nitrides $Ti_{n+1}C_n$, $Ti_{n+1}N_n$ (n=1, 2, and 3) from de-intercalated MAX phases: First-principles probing of their structural, electronic properties and relative stability. *Computational Materials Science* **2012**, 65, 104-114.
24. Shein, I. R.; Ivanovskii, A. L. Planar nano-block structures $Ti_{n+1}Al_{0.5}C_n$ and $Ti_{n+1}C_n$ (n=1, and 2) from MAX phases: Structural, electronic properties and relative stability from first principles calculations. *Superlattices and Microstructures* **2012**, 52, 147-157.
25. Enyashin, A. N.; Ivanovskii, A. L. Two-dimensional titanium carbonitrides and their hydroxylated derivatives: Structural, electronic properties and stability of MXenes $Ti_3C_{2-x}N_x(OH)_2$ from DFTB calculations. *Journal of Solid State Chemistry* **2013**, 207, 42-48.
26. Ivanovskii, A. L.; Enyashin, A. N. Graphene-like transition-metal nanocarbides and nanonitrides. *Russian Chemical Reviews* **2013**, 82, 735.
27. Khazaei, M.; Arai, M.; Sasaki, T.; Chung, C. Y.; Venkataramanan, N. S.; Estili, M.; Sakka, Y.; Kawazoe, Y. Novel Electronic and Magnetic Properties of Two-Dimensional Transition Metal Carbides and Nitrides. *Advanced Functional Materials* **2013**, 23, 2185-2192.
28. Khazaei, M.; Arai, M.; Sasaki, T.; Estili, M.; Sakka, Y. The effect of the interlayer element on the exfoliation of layered Mo_2AC (A = Al, Si, P, Ga, Ge, As or In) MAX phases into two-dimensional Mo2C nanosheets. *Science and Technology of Advanced Materials* **2014**, 15, 014208.
29. Khazaei, M.; Arai, M.; Sasaki, T.; Estili, M.; Sakka, Y. Two-dimensional molybdenum carbides: potential thermoelectric materials of the MXene family. *Physical Chemistry Chemical Physics* **2014**, 16, 7841-7849.
30. Mauchamp, V.; Bugnet, M.; Bellido, E. P.; Botton, G. A.; Moreau, P.; Magne, D.; Naguib, M.; Cabioc'h, T.; Barsoum, M. W. Enhanced and tunable surface plasmons in

two-dimensional Ti_3C_2 stacks: Electronic structure versus boundary effects. *Physical Review B* **2014**, 89, 235428.
31. Dall'Agnese, Y.; Lukatskaya, M. R.; Cook, K. M.; Taberna, P.-L.; Gogotsi, Y.; Simon, P. High capacitance of surface-modified 2D titanium carbide in acidic electrolyte. *Electrochemistry Communications* **2014**, 48, 118-122.
32. Liang, X.; Garsuch, A.; Nazar, L. F. Sulfur Cathodes Based on Conductive MXene Nanosheets for High-Performance Lithium–Sulfur Batteries. *Angewandte Chemie* **2015**, In Press.
33. Yang, E.; Ji, H.; Kim, J.; Kim, H.; Jung, Y. Exploring the possibilities of two-dimensional transition metal carbides as anode material for sodium batteries. *Physical Chemistry Chemical Physics* **2015**.
34. Lee, Y.; Hwang, Y.; Cho, S. B.; Chung, Y.-C. Achieving a direct band gap in oxygen functionalized-monolayer scandium carbide by applying an electric field. *Physical Chemistry Chemical Physics* **2014**, 16, 26273-26278.
35. Hu, J.; Xu, B.; Ouyang, C.; Yang, S. A.; Yao, Y. Investigations on V_2C and V_2CX_2 (X = F, OH) Monolayer as a Promising Anode Material for Li Ion Batteries from First-Principles Calculations. *The Journal of Physical Chemistry C* **2014**, 118, 24274-24281.
36. Lashgari, H.; Abolhassani, M. R.; Boochani, A.; Elahi, S. M.; Khodadadi, J. Electronic and optical properties of 2D graphene-like compounds titanium carbides and nitrides: DFT calculations. *Solid State Communications* **2014**, 195, 61-69.
37. Halim, J.; Lukatskaya, M. R.; Cook, K. M.; Lu, J.; Smith, C. R.; Näslund, L.-Å.; May, S. J.; Hultman, L.; Gogotsi, Y.; Eklund, P.; Barsoum, M. W. Transparent Conductive Two-Dimensional Titanium Carbide Epitaxial Thin Films. *Chem. Mater.* **2014**, 26, 2374-2381.
38. Eames, C.; Islam, M. S. Ion Intercalation into Two-Dimensional Transition-Metal Carbides: Global Screening for New High Capacity Battery Materials. *Journal of the American Chemical Society* **2014**, 136, 16270-16276.
39. Xie, Y.; Kent, P. R. C. Hybrid density functional study of structural and electronic properties of functionalized $Ti_{n+1}X_n$ (X=C, N) monolayers. *Physical Review B* **2013**, 87, 235441.
40. Gan, L.-Y.; Zhao, Y.-J.; Huang, D.; Schwingenschlögl, U. First-principles analysis of MoS_2/Ti_2C and MoS_2/Ti_2CY_2 (Y=F and OH) all-2D semiconductor/metal contacts. *Physical Review B* **2013**, 87, 245307.
41. Gan, L.-Y.; Huang, D.; Schwingenschlogl, U. Oxygen adsorption and dissociation during the oxidation of monolayer Ti_2C. *Journal of Materials Chemistry A* **2013**, 1, 13672-13678.
42. Lee, C.; Wei, X.; Kysar, J. W.; Hone, J. Measurement of the Elastic Properties and Intrinsic Strength of Monolayer Graphene. *Science* **2008**, 321, 385-388.
43. Bertolazzi, S.; Brivio, J.; Kis, A. Stretching and Breaking of Ultrathin MoS2. *ACS Nano* **2011**, 5, 9703-9709.
44. Lee, C.; Wei, X.; Li, Q.; Carpick, R.; Kysar, J. W.; Hone, J. Elastic and frictional properties of graphene. *physica status solidi (b)* **2009**, 246, 2562-2567.
45. Poot, M.; van der Zant, H. S. J. Nanomechanical properties of few-layer graphene membranes. *Applied Physics Letters* **2008**, 92, 063111.
46. Naguib, M.; Mochalin, V. N.; Barsoum, M. W.; Gogotsi, Y. MXenes: A New Family of Two-Dimensional Materials. *Adv. Mater.* **2014**, 26, 982-982.

47. Kurtoglu, M.; Naguib, M.; Gogotsi, Y.; Barsoum, M. W. First principles study of two-dimensional early transition metal carbides. *MRS Communications* **2012**, 2, 133-137.
48. Er, D.; Li, J.; Naguib, M.; Gogotsi, Y.; Shenoy, V. B. In *Mxenes As High Capacity Electrodes Materials for Metal (Li, Na, K, Ca)-Ion Batteries*, Meeting Abstracts, The Electrochemical Society: **2014**; pp 101-101.
49. Gan, L.-Y.; Zhao, Y.-J.; Huang, D.; Schwingenschlögl, U. First-principles analysis of MoS 2/Ti 2 C and MoS 2/Ti 2 C Y 2 (Y= F and OH) all-2D semiconductor/metal contacts. *Phys. Rev. B* **2013**, 87, 245307.
50. Borysiuk, V. N.; Mochalin, V. N.; Gogotsi, Y. Molecular dynamic study of the mechanical properties of two-dimensional titanium carbides Tin+ 1Cn (MXenes). *Nanotechnology* **2015**, 26, 265705.
51. Naguib, M.; Kurtoglu, M.; Presser, V.; Lu, J.; Niu, J. J.; Heon, M.; Hultman, L.; Gogotsi, Y.; Barsoum, M. W. Two-Dimensional Nanocrystals Produced by Exfoliation of Ti_3AlC_2. *Advanced Materials* **2011**, 23, 4248-4253.
52. Naguib, M.; Mochalin, V. N.; Barsoum, M. W.; Gogotsi, Y. 25th Anniversary Article: MXenes: A New Family of Two-Dimensional Materials. *Advanced Materials* **2014**, 26, 992-1005.
53. Xie, Y.; Kent, P. R. C. Hybrid density functional study of structural and electronic properties of functionalized $Ti_{n+1}X_n$ (X=C, N) monolayers. *Physical Review B* **2013**, 87.
54. Pei, Q. X.; Zhang, Y. W.; Shenoy, V. B. A molecular dynamics study of the mechanical properties of hydrogen functionalized graphene. *Carbon* **2010**, 48, 898-904.
55. Barsoum, M. W.; Radovic, M. Elastic and Mechanical Properties of the MAX Phases. *Annual Review of Materials Research, Vol 41* **2011**, 41, 195-227.
56. Tang, Q.; Zhou, Z.; Shen, P. W. Are MXenes Promising Anode Materials for Li Ion Batteries? Computational Studies on Electronic Properties and Li Storage Capability of Ti_3C_2 and $Ti_3C_2X_2$ (X = F, OH) Monolayer. *Journal of the American Chemical Society* **2012**, 134, 16909-16916.
57. Zhou, X. W.; Wadley, H. N. G.; Johnson, R. A.; Larson, D. J.; Tabat, N.; Cerezo, A.; Petford-Long, A. K.; Smith, G. D. W.; Clifton, P. H.; Martens, R. L.; Kelly, T. F. Atomic scale structure of sputtered metal multilayers. *Acta Materialia* **2001**, 49, 4005-4015.
58. Francis, M. F.; Neurock, M. N.; Zhou, X. W.; Quan, J. J.; Wadley, H. N. G.; Webb, E. B. Atomic assembly of Cu/Ta multilayers: Surface roughness, grain structure, misfit dislocations, and amorphization. *Journal of Applied Physics* **2008**, 104.
59. Zou, W.; Wadley, H. N. G.; Zhou, X. W.; Ghosal, S.; Kosut, R.; Brownell, D. Growth of giant magnetoresistance multilayers: Effects of processing conditions during radio-frequency diode deposition. *Journal of Vacuum Science & Technology a-Vacuum Surfaces and Films* **2001**, 19, 2414-2424.
60. Oymak, H.; Erkoc, F. Titanium coverage on a single-wall carbon nanotube: molecular dynamics simulations. *Chemical Physics* **2004**, 300, 277-283.
61. Berendsen, H. J. C.; Postma, J. P. M.; Vangunsteren, W. F.; Dinola, A.; Haak, J. R. Molecular-Dynamics with Coupling to an External Bath. *Journal of Chemical Physics* **1984**, 81, 3684-3690.
62. Anasori, B.; Halim, J.; Lu, J.; Voigt, C. A.; Hultman, L.; Barsoum, M. W. Mo_2TiAlC_2: A new ordered layered ternary carbide. *Scripta Mater.* **2015**, 101, 5-7.